

Electronic structure of GaN codoped with Mn and Cr

Nandan Tandon,¹ G. P. Das,² and Anjali Kshirsagar^{1,*}

¹*Department of Physics, University of Pune, Pune 411 007, India*

²*Department of Material Science, Indian Association for the Cultivation of Science, Jadavpur, Kolkata 700032, India*

(Received 13 March 2008; revised manuscript received 8 April 2008; published 22 May 2008)

We have studied the spin-polarized electronic structure of GaN codoped with transition metal (TM) atoms Mn and Cr, with different possible geometrical sites for the dopants, to determine the most favored geometry. The variations in the band structure, density of states, and TM site magnetic moment are analyzed for these geometries. Parallel and antiparallel spin configurations are energetically compared for all the geometries and it is observed that the parallel spin configuration with near neighbor substitution of TM atoms is the most favorable. Our results indicate that Ga(MnCr)N is a prospective candidate as a spintronics material to work at room temperature.

DOI: [10.1103/PhysRevB.77.205206](https://doi.org/10.1103/PhysRevB.77.205206)

PACS number(s): 71.20.-b, 71.55.Eq, 75.50.Pp

I. INTRODUCTION

The quest for a higher data density in information storage has motivated investigations beyond the conventional semiconductors based on electron-hole transport and normal magnetic materials recording information using electron spin. In order to exploit the use of the charge as well as the spin degrees of freedom of carriers near room temperature, investigations of the spintronics materials based on GaN, GaAs, CdTe, ZnTe, etc., are underway. The initial thrust was on semiconductors doped with single transition metal (TM) species, which is now culminating into codoping of semiconductors, either with magnetic materials or with cations and anions with one more or one less valence electron, to investigate newer materials for spintronics.

Over the past few years, a lot of attention has been focused on GaAs based diluted magnetic semiconductors (DMSs). (Ga,Mn)As based devices are realized by combining alternate ferromagnetic and nonmagnetic layers, and spin injection was experimentally demonstrated. However, it is confirmed in these experiments that the Curie temperature (T_C) of such DMS materials is only as high as 110 K.¹ Recently, there was a report of a T_C value at around 180 K observed for (Ga,Mn)As by annealing procedures by keeping the compensation effects minimal.²

Dietl *et al.*³ used the Zener model to theoretically explain ferromagnetism in DMS and also predicted materials that can have T_C above room temperature. In agreement with their prediction, group III-nitride semiconductors doped with 3d TMs such as Mn or Cr showed ferromagnetism with high T_C . Also, the (Ga,Mn)N system is preferable over (Ga,Mn)As because its band structure is much more suitable for spin injection.⁴ Theodoropolou *et al.* reported ferromagnetism in (Ga,Mn)N with a $T_C=250$ K.⁵ An estimation of T_C as high as 940 K in (Ga,Mn)N at 9% dopant concentration was reported in Mn-doped GaN grown on a sapphire substrate by using molecular-beam epitaxy.⁶ Mn-doped GaN in the form of thin films produced by varying the growth and annealing conditions showed Curie temperatures between 228 and 370 K.⁷ The addition of Cr in GaN single crystals grown by the flux method was reported to show $T_C=280$ K.⁸ (Ga,Cr)N layers grown on sapphire substrates

by electron-cyclotron-resonance plasma-assisted molecular-beam epitaxy showed ferromagnetism at temperatures above 400 K.⁹ Ion implanted Cr in *p*-type GaN showed magnetization above 300 K, as reported by Lee *et al.*¹⁰ Such DMSs, with larger band gaps and smaller lattice constants as compared to GaAs based DMSs, have become the focus of attention because of their potential as room temperature spintronics materials. A reasonably high concentration of d^n impurity, such as Mn^{2+} , with a high concentration of holes as carriers mediating the magnetic coupling, is the likely cause of the high T_C . The lattice location and distribution of the individual localized moments due to the dopant atoms critically affect the magnetic coupling. Mn-doped GaN was studied by Sanyal *et al.*¹¹ by using first principles plane wave method, wherein they saw the effect of varying the Mn concentration on the electronic and magnetic properties. First principles tight-binding linearized muffin-tin orbital (TB-LMTO) calculations indicated that the coupling between Mn and Cr atoms is ferromagnetic whether they are doped in the crystal or in cluster.^{12,13}

It is observed that GaN doped purely with Mn or Cr shows high T_C with the magnetic moment at the TM site in the Mn-doped system higher compared to that in the Cr-doped system.¹⁴ However, the minority spin gap for TM d states in the pure Cr-doped system is higher (3 eV) compared to that in the pure Mn-doped system (2 eV), and this is an important fact from the application point of view. We conjecture that systems codoped with Mn and Cr might show better properties for spintronics applications. Therefore, in the present work, we incorporate both Mn and Cr in the semiconductor host GaN. The interactions between the localized magnetic moments, which are introduced by the Mn and Cr atoms in the GaN host, are of significance from the spintronics material point of view. The systematics are studied by varying the distance between the dopant atoms to signify the changes in the interaction among the dopant atoms as well as that between the dopant and valence electrons of the host system and to realize the most favorable configuration.

II. METHOD AND COMPUTATIONAL DETAILS

We use the full potential linear augmented plane wave method as implemented in the WIEN2K package¹⁵ with a gen-

eralized gradient approximation for the exchange correlation energy functional as parametrized by Perdew *et al.*¹⁶ We analyzed systems with one Mn and one Cr (Mn+Cr) doped in a 32 atom GaN supercell, amounting to 12.5% doping. Since the structure of GaN is wurtzite, there are many inequivalent sites with different distributions of near neighbors. Various such inequivalent geometries of dopants are studied with the minimum and maximum distances between the dopants of ~ 3.19 and ~ 6.0 Å, respectively. However, in the present work, we depict the results for two geometries expressing the substitution of TM impurities with a Mn-Cr distance of 3.19 Å as near neighbor (nn) and that of 5.2 Å as distant neighbor (dn). More computational details and the geometries considered during the study are described in detail in our previous work.¹⁴ Since the calculations are done within the supercell approach, we have also carried out limited calculations for a 72 atom unit cell to understand the effect of the supercell size. We have calculated the heat of formation (FE) for various substitutionally doped systems by using the following relation:

$$FE = E(\text{Ga}_{16-x-y}\text{Mn}_x\text{Cr}_y\text{N}_{16}) - \{(16-x-y)E(\text{Ga, bulk}) + 16[E(\text{N, bulk})] + x[E(\text{Mn, bulk})] + y[E(\text{Cr, bulk})]\}, \quad (1)$$

where $E(\text{Ga}_{16-x-y}\text{Mn}_x\text{Cr}_y\text{N}_{16})$ is the total energy per unit cell and $E(A, \text{bulk})$ denotes the energy per atom of substance A .

III. RESULTS

A. Vacancy and pure doped systems

It has been theoretically reported earlier that the TM atom prefers the substitutional site than the interstitial site in the host GaN.¹⁷ Wang *et al.*¹⁸ observed temperature-dependent photoluminescence (PL) spectra of Cr-implanted GaN, which imply that Cr substitutionally incorporates on the Ga site and forms a deep acceptor level in GaN.¹⁸ Similarly, Jeon *et al.*¹⁹ indicated from band edge exciton transitions in $\text{Ga}_{1-x}\text{Mn}_x\text{N}$ thin films that Mn atoms act as substituents. Hence, in our calculations, the TM atoms are substituted at the Ga sites. We have calculated the electronic structure of GaN with one and two vacancies to know the states that will hybridize when a vacancy is filled with a TM atom. These results aid in analyzing and understanding the results for doped systems.

GaN is a spin compensated semiconductor with the valence band consisting of N p states and the Ga s states forming a well separated lowest conduction band. The introduction of a vacancy introduces imbalance in the two spin channels. A spin-polarized band structure calculation for GaN with a Ga vacancy (V_{Ga}) is seen to introduce three acceptor states in the system that lie in a window with a width of about 1 eV above the valence N p band. A comparison of the site projected density of states (DOS) at different N sites in a vacancy system is depicted in Fig. 1(a). The up spin DOS is not very different from that in pure GaN; however, the down spin DOS extends beyond the Fermi level. The triple acceptor states are split into a doublet and a singlet. The doublet is formed from a combination of dangling

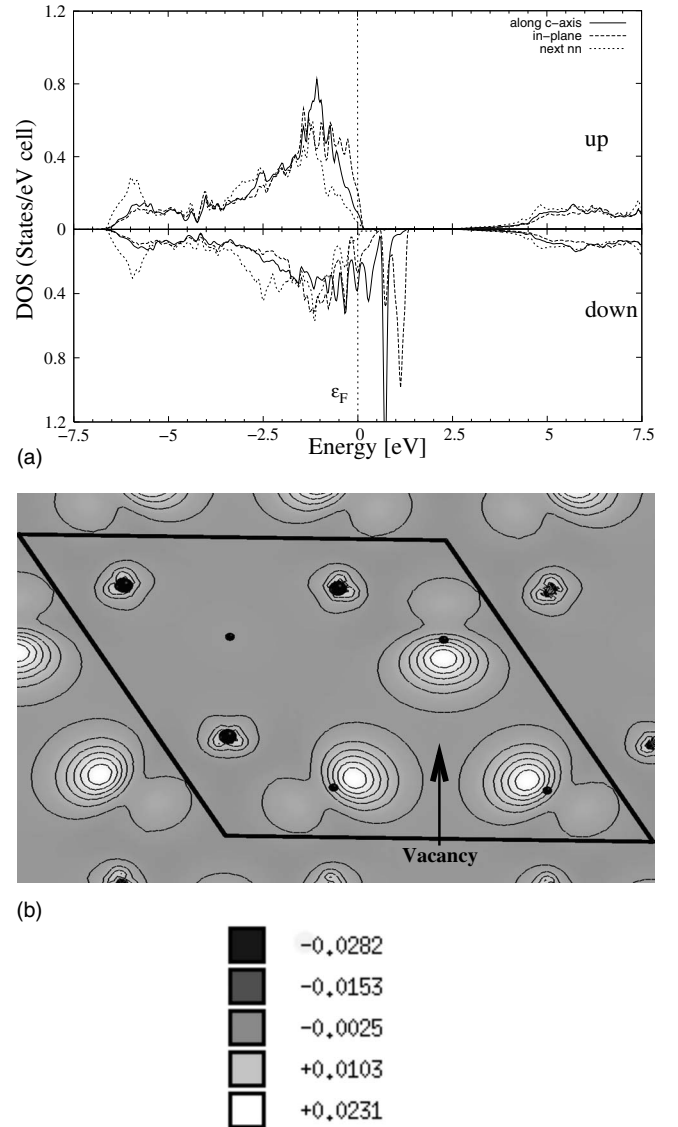


FIG. 1. (a) Site projected DOS of N atoms in the vacancy system. The upper panel shows the DOS for up spin and the lower panel shows that for down spin. The vacancy is surrounded by four N atoms; three N atoms form a plane and the fourth N atom lies above the vacancy site along the c axis. The full line is for nn N atom along the c axis, the dashed line is for nn N atom in the N plane, and the dotted line is for a distant N atom. The up spin DOS for the distant N atom is almost similar to the DOS of the N atom in pure GaN. Although the up and down spin DOSs are identical in pure GaN, the down spin DOS shows the influence of the vacancy on the N DOS in the vacancy system. (b) Contour plots of SCD in a plane containing the vacancy and Ga atoms. The large filled circles represent Ga atoms and the maximum negative SCD is seen on these atoms. The small filled circles are N atoms. The maximum in the SCD is shifted away from the near neighbor N atoms toward the vacancy site.

bonds of three equivalent N neighbors lying in plane with the vacancy and the singlet is located on the N atom situated along the c axis above the vacancy site.²⁰ This is reflected in the spin charge density (SCD) plot shown in Fig. 1(b). SCD is positive near the vacancy site, indicating empty down spin

levels. These three acceptor states in the minority spin are the ones that will be affected and are therefore expected to contribute to bonding with TM bands. On substitution of TM atom at the V_{Ga} site, the electrons from the TM atom will fill the minority p states of N atoms. The Ga atom that is removed to create a vacancy is one of the four near neighbors for four N atoms tetrahedrally bonded to it. In pure GaN, the Ga $3s$ and $3p$ levels are known to form the low lying conduction bands. However, these s bands are seen to hybridize with the N $2s$ and $2p$ bands. Therefore, GaN has partly ionic and partly covalent bonding. Removal of one Ga atom takes away three electrons from the valence band of GaN. This fact introduces a disparity in the spin-up and spin-down bands.

When a TM atom is substituted at the cationic site, its fivefold degenerate d levels split into threefold degenerate t_2 and doubly degenerate e levels, with the T_d group symmetry for a TM atom tetrahedrally bonded to four N atoms. For TM substituted at the Ga site in the GaN crystal, the point group symmetry is further reduced to D_{4h} and e levels split into $a_{1g}(3z^2-r^2)$ and $b_{1g}(x^2-y^2)$ and t_2 levels split into $b_{2g}(xy)$ and $e_g(xz, yz)$. In our earlier work,¹⁴ we saw that two bands have accidental degeneracy at the Γ point for Mn substitution and at the K point for Cr substitution and we used the nomenclature $a_{1\uparrow}(3z^2-r^2)$, $e_{1\uparrow}(xz, yz)$, and $e_{2\uparrow}(x^2-y^2, xy)$ for these bands with a majority spin. Thus, in the single Mn doping, the Mn d bands split into $e_{1\uparrow}$, $a_{1\uparrow}$ (which are filled), and $e_{2\uparrow}$ (which is half filled). The Cr d bands in $\text{Ga}_{15}\text{CrN}_{16}$ are $e_{1\uparrow}$ (which lies below E_F), $a_{1\uparrow}$, and $e_{2\uparrow}$ (which are partially occupied).¹⁴ Thus, in the case of single Mn doping, two electrons from the $4s$ and one electron from the $3d$ levels occupy the acceptor states and thus introduce one hole. Similarly, single Cr-doping introduces two holes. When we put one Mn and one Cr atom in a unit cell, they introduce three holes in the system with the E_F lying amidst the majority impurity d band. It is to be noted that V_{Ga} , too, introduces three hole states.

Figures 2(a)–2(c) show Mn derived d states in $\text{Ga}_{15}\text{MnN}_{16}$, $\text{Ga}_{14}\text{Mn}_2\text{N}_{16}$, and $\text{Ga}_{14}\text{CrMnN}_{16}$, respectively, at nn substitution in the latter two cases. It is clearly visible that the bands formed around Fermi level (E_F) are purely due to the presence of TM impurity in the GaN host. In going from one Mn atom to two Mn atoms, the number of Mn d states doubles and the width of the band also increases. This broadening of partially filled d states stabilizes the ferromagnetism through a double exchange interaction.^{21,22} These TM derived d states hybridize with the s and p states of N. This hybridization is seen to decrease in going from $\text{Ga}_{15}\text{MnN}_{16}$ to $\text{Ga}_{14}\text{Mn}_2\text{N}_{16}$ from the site projected DOS (not shown here) but does not disappear altogether. Figures 2(d)–2(f) show the majority spin impurity d bands of Cr substituted in $\text{Ga}_{15}\text{CrN}_{16}$, $\text{Ga}_{14}\text{Cr}_2\text{N}_{16}$, and $\text{Ga}_{14}\text{CrMnN}_{16}$, respectively, at nn substitution in the latter two cases. The nature of the occupied states of Cr, viz., $e_{1\uparrow}$, remains almost the same in the three systems. The partially filled $e_{2\uparrow}$ and $a_{1\uparrow}$ are more delocalized, indicating d - d hybridization in systems with more than one Cr impurity. In pure Cr-doped systems, the hybridization of TM d states with N s and p states is drastically reduced in more than one TM atom per unit cell. The partially filled $e_{2\uparrow}$ states are present in both the systems. We

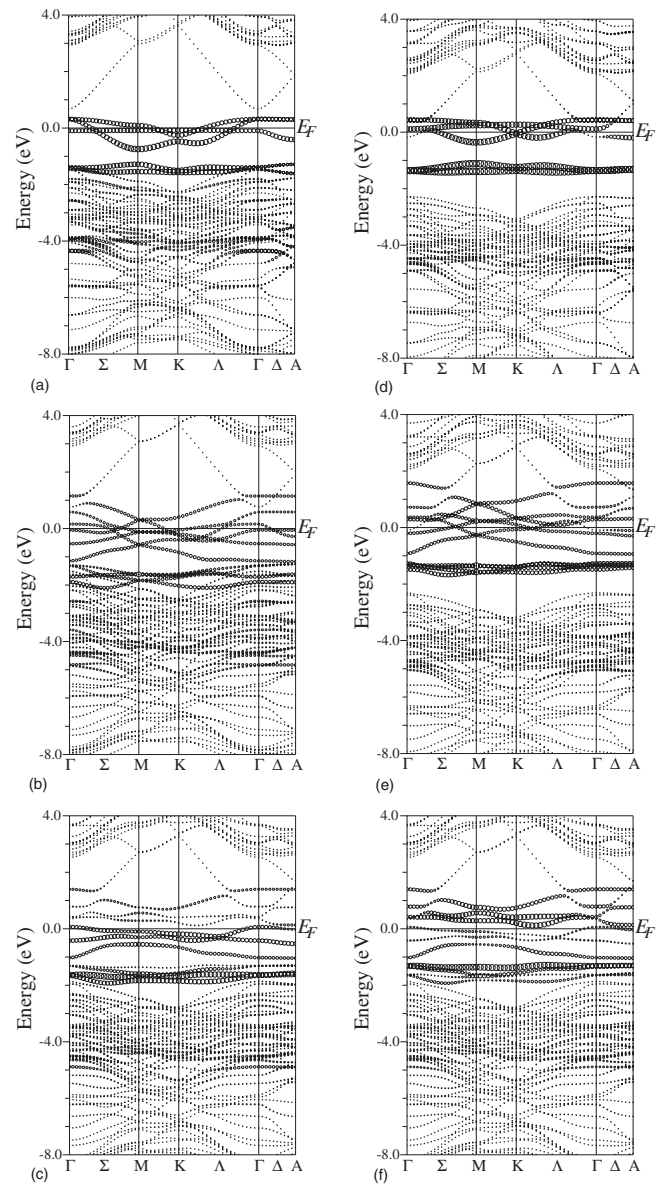


FIG. 2. Majority d bands of Mn in (a) $\text{Ga}_{15}\text{MnN}_{16}$, (b) $\text{Ga}_{14}\text{Mn}_2\text{N}_{16}$, and (c) $\text{Ga}_{14}\text{CrMnN}_{16}$, and Cr in (d) $\text{Ga}_{15}\text{CrN}_{16}$, (e) $\text{Ga}_{14}\text{Cr}_2\text{N}_{16}$, and (f) $\text{Ga}_{14}\text{CrMnN}_{16}$.

see that the levels are closer to the host states in the Mn-doped system than those in the Cr-doped system.

The energy level diagrams for the majority spin states are schematically represented for single Mn and single Cr substitution in GaN in Figs. 3(a) and 3(b), respectively. Mn and Cr form deep acceptor bands when substituted in GaN. Mn derived bands lie closer to the valence band maximum (VBM) than the Cr derived bands, which lie about 1 eV above the VBM. The hybridization of Mn d states with VBM is more than that of Cr d states, and thus, the Cr d bands are more localized as compared to Mn d bands. Cr states are delocalized in two atom substituted systems in comparison to single impurity doping; however, in comparison to Mn, they are more localized even in a two atom doping configuration. When two Mn or two Cr atoms are substituted at nn sites, the bonding and antibonding states resulting from d - d hybridiza-

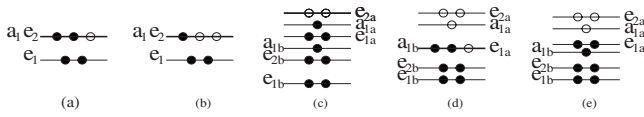


FIG. 3. Schematic of TM impurity levels for various systems (not to scale): (a) single Mn-doping, (b) single Cr-doping, (c) nn doping of two Mn atoms, (d) nn doping of two Cr atoms, and (e) nn doping of one Mn and one Cr atom. The levels lying close in energy are shown by thick lines.

tion are schematically shown in Figs. 3(c) and 3(d), respectively, based on the site projected majority spin bands and DOS.¹⁴ It is seen that the VBM of host GaN is below the TM d states with holes in the impurity band. When the system has holes at the top of the d band, instead of the p - d hybridization, it is the d - d coupling that stabilizes the ferromagnetic or antiferromagnetic state. This indicates a double exchange interaction in pure doped systems.

B. Mn-Cr codoped systems

1. Electronic structure

Figures 2(c) and 2(f) respectively show nn substituted Mn and Cr site projected majority spin bands in $\text{Ga}_{14}\text{CrMnN}_{16}$. The Mn bands are present just above the VBM of GaN and the Cr levels are ~ 0.6 eV above the VBM. In the case of $\text{Ga}_{14}\text{CrMnN}_{16}$, as seen in Fig. 2(c), the hybridized Mn d bands lie below E_F and are almost completely filled. The Cr $a_{1\uparrow}$ and $e_{2\uparrow}$, which are partially occupied in pure Cr-doped systems, lie above E_F , as can be seen in Fig. 2(f), whereas the Cr $e_{1\uparrow}$ is occupied. The Mn and Cr levels hybridize such that the bonding levels e_{1b} , e_{2b} , and a_{1b} and antibonding level e_{1a} are filled, as shown in Fig. 3(e). Bonding states dominantly have Mn d character, while antibonding states primarily consist of Cr d states. TM d and host p state hybridization does not seem to be affected.

Figures 4 and 5 show the site projected d DOSs at the Mn and Cr sites in $\text{Ga}_{14}\text{CrMnN}_{16}$ for Cr-Mn distances of ~ 3.19 and ~ 5.2 Å, respectively. The DOS curves depict a half-metallic nature with 100% spin polarization for both the distances, as is observed for pure Mn- and/or Cr-doping, although the details of the d DOS in the majority spin are different for nn substitution. Half-metallicity is very important for an efficient spin injection. For doping at dn sites, the DOS does not differ much from that observed in the pure Mn or Cr doping at 5.2 Å, indicating that the extent of interaction between the TM atoms is less. The minority levels are more localized at dn substitution. The effect of Cr codoping on the minority spin levels is to shift the Mn derived states in the valence band to the left and in the conduction band to the right of E_F , thus increasing the exchange splitting of Mn d bands in comparison to the pure Mn-doped system. However, as desired, the minority spin gap for $\text{Ga}_{14}\text{CrMnN}_{16}$ does not increase; it remains around ~ 2.0 eV. We thus see that (i) the hybridization of Mn and Cr states leads to impurity states in proximity to E_F and, therefore, a free flow of charge carriers between the impurities and host and (ii) although the band gap for the minority spin does not increase,

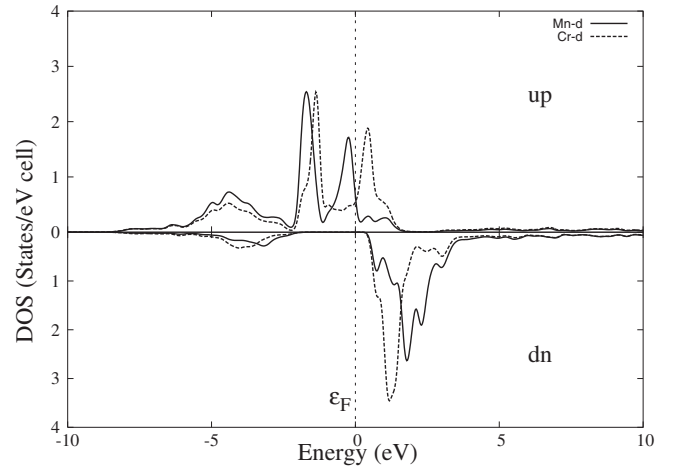


FIG. 4. Site projected TM d DOS in $\text{Ga}_{14}\text{CrMnN}_{16}$, wherein the Mn-Cr distance is ~ 3.19 Å.

the exchange splitting of TM d states increases. This suggests that the codoped system could be possibly a better candidate for spintronics applications.

We find that among the Mn+Cr systems that we studied, the lowest energy geometry is the case in which the Mn-Cr distance is 3.19 Å. This suggests that even in the codoping case, the clustering of Mn-Cr atoms is favored, as observed in the pure Mn- or pure Cr-doping case. However, it may be noted that all the calculations reported are only for two TM atom substitution in a unit cell. Thus, with more TM atoms, the results might be different.

2. Magnetism

The total magnetic moment per unit cell for the $\text{Ga}_{14}\text{CrMnN}_{16}$ system is $7\mu_B$ for all the Mn-Cr distances, as depicted in Table I. With codoping at nn distance, the magnetic moment at the Mn site increased from a value of $3.34\mu_B$ for the pure Mn-doped system to $3.54\mu_B$ and reduced to a value of $2.25\mu_B$ at the Cr site from a value of $2.47\mu_B$ in the pure Cr-doped system. The magnetic moment on near

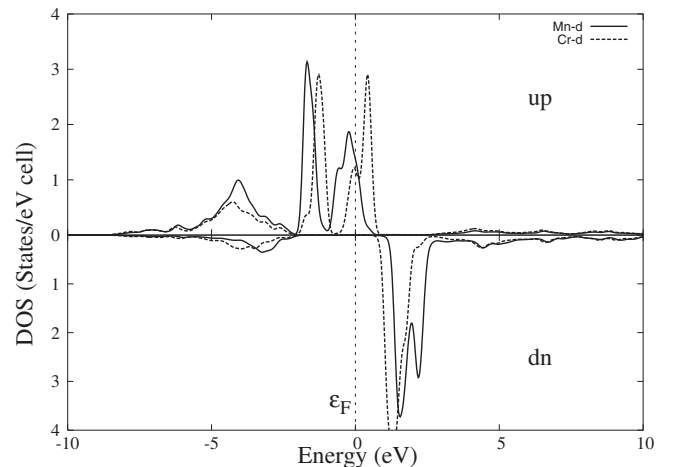


FIG. 5. Site projected TM d DOS in $\text{Ga}_{14}\text{CrMnN}_{16}$, wherein the Mn-Cr distance is ~ 5.2 Å.

TABLE I. Magnetic moment (μ_B) for various geometries of TM atoms in $\text{Ga}_{14}\text{MnCrN}_{16}$. $\text{Total}_{\text{mom}}$ indicates the magnetic moment per unit cell, Mn_{mom} is the magnetic moment at the Mn site, and Cr_{mom} is the magnetic moment at the Cr site.

Mn-Cr distance (\AA)	$\text{Total}_{\text{mom}}$	Mn_{mom}	Cr_{mom}
3.19	7.00	3.54	2.25
4.50	7.00	3.49	2.31
5.19	7.00	3.49	2.32
6.00	7.00	3.49	2.34

neighbor N atoms of Mn is observed to marginally increase. This could be attributed to an increase in hybridization of Mn states with the neighboring N atom states, as seen from the band structure plots. In the codoped system, the Mn majority spin states are completely filled, whereas, except for $e_{1\uparrow}$, all of the Cr majority states are empty, indicating charge transfer from Cr to Mn.

A few conclusions can be drawn about the magnetic interaction present in this type of DMS. The DOS and band structure plots show that the acceptor levels created by the TM impurity atoms are deep in the gap region of the host semiconductor. The E_F lies amidst the majority spin impurity d bands; the minority spin bands are pushed above E_F , forming the bottom of the conduction band. The impurity bands are partially filled and the widths of the d bands are smaller than the exchange splitting. This nature of the band structure and DOS is associated with the double exchange mechanism.²³

In the pure Mn-doped system, the d band is more than half-filled and E_F lies near the top of the impurity d band for the majority spin. On the other hand, for the pure Cr-doped system, the d band is less than half-filled and E_F lies in the lower half of the impurity d band for the majority spin. We observe that in the codoped system, E_F is located at the center of the impurity band. Thus, when the double exchange is dominant, ferromagnetism is more stable in the codoped system. Earlier reports ruled out hole and/or carrier-mediated ferromagnetism in GaN based DMSs doped with Mn or Cr.^{24,25} The same holds true for GaN codoped with Mn and Cr.

3. Structural stability and estimation of T_C

We have calculated the heat of formation, FE, for all the systems by using Eq. (1), which is given in Sec. II. The values are listed in Table II for various geometries. A negative value for all the systems indicates that the doped systems are stable. The codoped systems are less stable compared to the pure Mn-doped systems but are more stable compared to the pure Cr-doped systems.

The energy difference ΔE was estimated from the total energies for the two spin configurations, namely, parallel and antiparallel orientations of the localized magnetic moments on the doped TM atoms, for each geometry studied. Figure 6 shows the variation in ΔE for the different geometries of TM atoms for pure Mn, pure Cr, and codoped systems. For a system with two localized spin moments, the energy differ-

TABLE II. The heat of formation, FE, per unit cell (in Ry) for two substitutional TM atoms in a 32 atom unit cell.

Distance (\AA)	Pure Mn-doped	Pure Cr-doped	Mn-Cr codoped
3.19	-3.46	-3.37	-3.43
4.50	-3.42	-3.33	-3.39
5.19	-3.42	-3.33	-3.39
6.00	-3.43	-3.33	-3.39

ence ΔE is a measure of the exchange interaction J . The graph of ΔE vs dopant distance shows trends similar to that of J vs b/a in Fig. 1 of Ref. 26. Among the pure doped systems, the ferromagnetic (FM) state is most stable for pure Cr-doping (ΔE highest). ΔE for the codoped system is higher than that for the pure doped case for nn substitution. On increasing the distance between the substituted TM atoms, ΔE decreases from the nn configuration. The double exchange mechanism is thus strong and short ranged, as seen in Fig. 6. The dependence of ΔE on concentration of TM atoms could not be verified since the percentage of doping is kept constant in our work.

We have predicted the T_C for the $\text{Ga}_{14}\text{CrMnN}_{16}$ DMS system, as is done for the pure Mn- and pure Cr-doped cases^{14,27,28} within the mean field approximation (MFA). Although it is known that the Curie temperature is overestimated by MFA, because the model only considers linear dependence of ΔE and does not consider possible compensation effects within the system, a high ΔE will still imply a high T_C value.

The Mn-Cr codoped system has a T_C value higher than that of the pure Cr-doped system but lower than that of the pure Mn-doped system at nn substitution. It is clearly seen that the T_C is sensitive to the distribution of dopants. Since the experimentally measured T_C values for pure Mn or Cr-doped systems show a large distribution of temperatures, and this distribution includes the values predicted in the MFA,

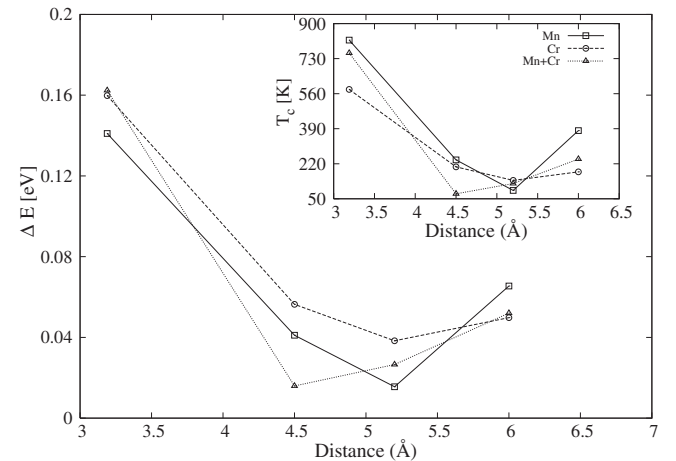


FIG. 6. $\Delta E = E_{\text{AFM}} - E_{\text{FM}}$ as a function of the distance between dopants for pure Mn (continuous line through squares), pure Cr (dashed line through circles), and one Mn+one Cr (dotted line through triangles) case. The inset shows the variation in T_C with distance.

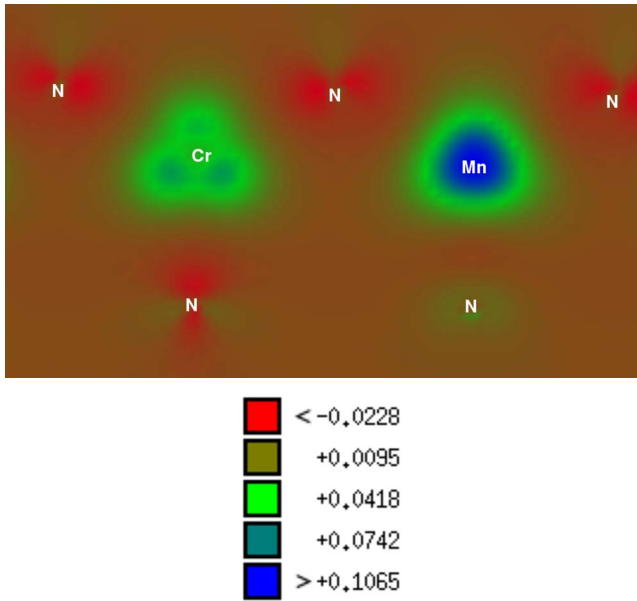


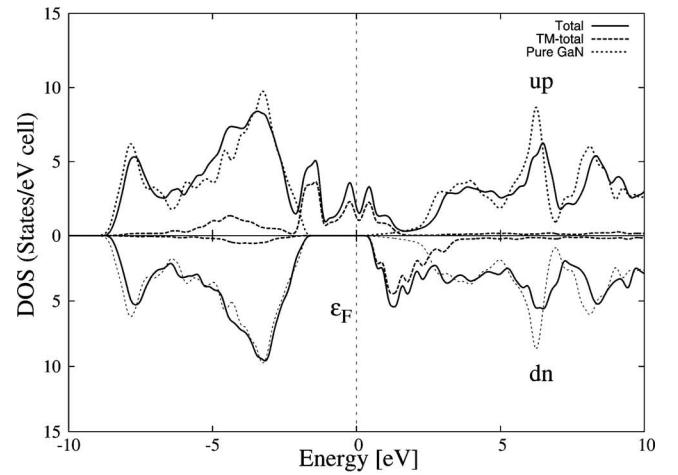
FIG. 7. (Color online) SCD plot in a plane containing two nearest N atoms from the plane above the cation and two nearest N atoms from the plane below the cations for nn substitution of the TM atoms in $\text{Ga}_{14}\text{CrMnN}_{16}$.

one would also expect the same for one Mn+one Cr-doped systems.

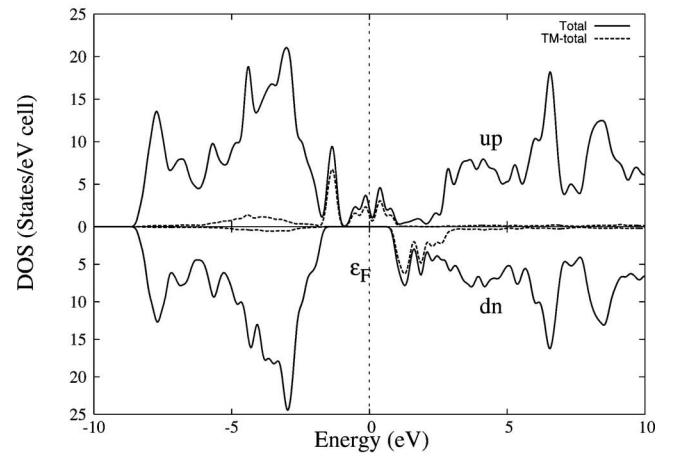
Xu *et al.*²⁹ used a local spin-density approximation combined with a linear response technique to map the magnetic energy onto a Heisenberg Hamiltonian. They showed that ferromagnetism in DMS is sensitive to configurational disorder, in particular, ordering increases T_C , while clustering decreases T_C . The ordering of DMSs is influenced by magnetic percolation and the measured T_C values are therefore sensitive to details of sample preparation, which is in agreement with observations. We expect that clustering will be less probable in the codoped system than in the pure Mn-doped system and, therefore, may affect the T_C value in practice.

4. Charge density analysis

The SCD on the nearest N atoms of the TM atoms in $\text{Ga}_{14}\text{CrMnN}_{16}$ is interesting to understand the interaction between the TM atoms. As seen in the pure Cr-doped DMS, the SCD on all the nearest N atoms is negative, giving an induced negative magnetic moment. In pure Mn doping, the SCD on nearest N atoms of Mn is positive. Similar observations were also experimentally made.^{30,31} In the case of nn doping of one Mn and one Cr, all nearest N atoms of Cr have negative SCD, as shown in Fig. 7. The N atoms, which are bonded to both Mn and Cr, have a negative SCD. The nearest N atom, lying along the c axis on top of the TM atom, has a positive SCD for Mn and a negative SCD for Cr. This is understood from Fig. 3(a), wherein the Mn $a_{1\uparrow}$ is occupied, whereas the Cr $a_{1\uparrow}$ [Fig. 3(b)] is empty, and thus, hybridization with N along the c axis is stronger in the case of Mn than that in Cr. The number of hole states in $\text{Ga}_{1-x}\text{Cr}_x\text{N}$ is more than that in $\text{Ga}_{1-x}\text{Mn}_x\text{N}$. Second, the hole states in Mn are less localized about the Mn atoms than the corresponding



(a)



(b)

FIG. 8. Total (continuous line) and transition metal (dashed line) DOSs in (a) $\text{Ga}_{14}\text{MnCrN}_{16}$ as well as the pure GaN DOS (dotted line) and (b) $\text{Ga}_{34}\text{MnCrN}_{36}$.

states in Cr in pure doped systems. Therefore, the sign of polarization on N atoms reflects the p - d interaction and will play a role in codoped systems. The overall average magnetic moment on nearest N atoms for a TM atom is positive for Mn and negative for Cr.

5. Large unit cell calculations

In order to verify that the FM configuration of dopants, which is energetically the most favored in a 32 atom unit cell, is indeed the global minimum and that the interactions between the dopants within one unit cell are not influenced by the dopants of the next unit cell, we performed limited calculations for a larger unit cell of 72 atoms. Substitution of two dopants at the cation sites in the 72 atom unit cell results in 5.5% doping, which is closer to the experimental values. Self-consistency was achieved for the system wherein the dopants were substituted at the nn sites; the next neighbor in the xy plane is at a distance of 6.38 Å and the first neighbor along the z axis is at a distance of 10.38 Å. Parallel as well as antiparallel orientations of localized magnetic moments on the TM atoms for the magnetic interaction of the dopants

were studied to find the lowest energy configuration. As in the 32 atom unit cell, the parallel configuration of spins at the Mn and Cr sites is lower in energy. The TM site magnetic moment on Mn is $3.53\mu_B$, which is comparable to that in the 32 atom unit cell and on Cr, it is $2.22\mu_B$ which is marginally lower than that in the 32 atom unit cell.

The DOS for pure $\text{Ga}_{16}\text{N}_{16}$ is shown in Fig. 8(a) (dotted line) for comparison with $\text{Ga}_{14}\text{MnCrN}_{16}$ DOS. As expected, the minority spin DOS is similar and is not influenced by the presence of TM atoms in the valence band. This also highlights the position of the TM levels with respect to the GaN levels very clearly.

Figures 8(a) and 8(b) show the total and TM site projected DOSs in a 32 atom unit cell and a 72 atom unit cell of $\text{Ga}_x\text{MnCrN}_y$, respectively. The half-metallic nature is seen in both the systems and the contribution to the states around E_F is clearly due to TM atoms. The character of the minority spin DOS is similar in the two cases. For the majority spin, the TM band just above the host VBM is broader in the case of the 32 atom unit cell, in comparison to the corresponding band in the 72 atom unit cell. It may be pointed out that among the two structures, the 32 atom unit cell has a higher concentration ($\sim 12\%$) of dopants and the broader d bands, which are clearly due to the TM atoms, are a consequence of this.

There are clearly two bands formed due to the impurity levels: one below E_F and the other around the E_F . A comparison of Figs. 8(a) and 8(b) indicates that with decreasing concentration of dopants, the $e_{1\uparrow}$ band will be more localized. The other two bands, $a_{1\uparrow}$ and $e_{2\uparrow}$, do not change much and remain partially (half in the codoped system) occupied. The magnitude of the TM site projected DOS is more or less the same in the two systems.

IV. CONCLUSIONS

In conclusion, we have studied the spin-polarized electronic structure of GaN codoped with Mn and Cr. We find

that such a material is a probable candidate for spintronics applications due to its half-metallic character and possibility of above room temperature transition temperature. The band structure is more favorable than that of the pure doped GaN for spin injection when put in a heterostructure. From experimental observations, the transition temperature T_C of the pure Mn-doped system is very sensitive to impurities, defects, or disorder in the system, while the pure Cr-doped systems are not so sensitive. We therefore feel that codoped systems will be better candidates. Another observation reports that Cr introduction increases paramagnetic contribution and we also find that for Mn+Cr systems, the ferromagnetic state is lower in energy than the pure Cr-doped system. On the other hand, in pure Mn-doped systems, clustering of Mn atoms takes place and this lowers T_C . An ordered ferromagnetic state is more probable in codoped systems. Sandratskii and Bruno³² showed that ferromagnetism in (Ga,Mn)As is very sensitive to the presence of donor defects such as As antisites.³² On the other hand, T_C for (Ga,Cr)As rather weakly depends on the presence of such impurities. However, it sharply decreases with decrease in the number of electrons. Experimentally, the formation of antisite defects is difficult to avoid in DMS materials. Hence, the need for a system that is less sensitive to defects and still has comparatively high T_C is essential. We hope that these calculations can motivate some experimentalists to work on TM codoped GaN systems.

ACKNOWLEDGMENTS

We thank BRNS, DAE, Government of India for financial support. A.K. acknowledges financial support from DST and UGC, Government of India. We acknowledge CMS, University of Pune, and IUCAA for the use of HPC facility. N.T. and A.K. acknowledge the hospitality of AS ICTP, Trieste, Italy.

*anjali@physics.unipune.ernet.in

¹H. Ohno, Science **281**, 951 (1998), and references therein.

²T. Jungwirth, K. Y. Wang, J. Masek, K. W. Edmonds, J. Konig, J. Sinova, M. Polini, N. A. Goncharuk, A. H. MacDonald, M. Sawicki, A. W. Rushforth, R. P. Campion, L. X. Zhao, C. T. Foxon, and B. L. Gallagher, Phys. Rev. B **72**, 165204 (2005).

³T. Dietl, H. Ohno, F. Matsukura, J. Cibert, and D. Ferrand, Science **287**, 1019 (2000).

⁴J. Kudrnovsky, I. Turek, V. Drchal, F. Maca, P. Weinberger, and P. Bruno, Phys. Rev. B **69**, 115208 (2004).

⁵N. Theodoropoulou, A. F. Hebard, M. E. Overberg, C. R. Abernathy, S. J. Pearton, S. N. G. Chu, and R. G. Wilson, Appl. Phys. Lett. **78**, 3475 (2001).

⁶T. Sasaki, S. Sonada, Y. Yamamoto, K. Suga, S. Shimizu, K. Kindo, and H. Hori, J. Appl. Phys. **91**, 7911 (2002).

⁷M. L. Reed, N. A. El-Masry, H. H. Stadelmaier, M. K. Ritums, M. J. Reed, C. A. Parker, and S. M. Bedair, Appl. Phys. Lett. **79**, 3473 (2001).

⁸S. E. Park, H. H. Lee, Y. C. Cho, S. Y. Jeong, C. R. Cho, and S. Cho, Appl. Phys. Lett. **80**, 4187 (2002).

⁹M. Hashimoto, Y. Zhou, M. Kanamura, and H. Asahi, Solid State Commun. **122**, 37 (2002).

¹⁰J. S. Lee, J. D. Lim, Z. G. Khim, Y. D. Park, S. J. Pearton, and S. N. G. Chu, J. Appl. Phys. **93**, 4512 (2003).

¹¹B. Sanyal, O. Bengone, and S. Mirbt, Phys. Rev. B **68**, 205210 (2003).

¹²G. P. Das, B. K. Rao, and P. Jena, Phys. Rev. B **68**, 035207 (2003).

¹³G. P. Das, B. K. Rao, and P. Jena, Phys. Rev. B **69**, 214422 (2004).

¹⁴N. Tandon, G. P. Das, and A. Kshirsagar, J. Phys.: Condens. Matter **18**, 9245 (2006).

¹⁵P. Blaha, K. Schwarz, G. K. H. Madsen, D. Kvasnicka, and J. Luitz, WIEN2k, An Augmented Plane Wave Plus Local Orbitals Program for Calculating Crystal Properties (Vienna University of Technology, Vienna, Austria, 2001).

- ¹⁶J. P. Perdew, K. Burke, and M. Ernzerhof, *Phys. Rev. Lett.* **77**, 3865 (1996).
- ¹⁷B. Sanyal and S. Mirbt, *J. Magn. Magn. Mater.* **290-291**, 1408 (2005).
- ¹⁸J. Wang, P. Chen, X. Guo, Z. Li, and W. Lu, *J. Cryst. Growth* **275**, 393 (2005).
- ¹⁹H. C. Jeon, J. A. Lee, Y. Shon, S. J. Lee, T. W. Kang, T. W. Kim, Y. K. Yeo, Y. H. Cho, and M. Kim, *J. Cryst. Growth* **278**, 671 (2005).
- ²⁰J. Neugebauer and C. G. Van de Walle, *Phys. Rev. B* **50**, 8067 (1994).
- ²¹H. Akai, *Phys. Rev. Lett.* **81**, 3002 (1998).
- ²²K. Sato and H. Katayama-Yoshida, *Semicond. Sci. Technol.* **17**, 367 (2002).
- ²³B. Belhadji, L. Bergqvist, R. Zeller, P. H. Dederichs, K. Sato, and H. Katayama-Yoshida, *J. Phys.: Condens. Matter* **19**, 436227 (2007).
- ²⁴J. J. Kim, H. Makino, K. Kobayashi, Y. Takata, T. Yamamoto, T. Hanada, M. W. Cho, E. Ikenaga, M. Yabashi, D. Miwa, Y. Nishino, K. Tamasaku, T. Ishikawa, S. Shin, and T. Yao, *Phys. Rev. B* **70**, 161315(R) (2004).
- ²⁵T. Graf, M. Gjukic, M. S. Brandt, and M. Stutzmann, *Appl. Phys. Lett.* **81**, 5159 (2002).
- ²⁶L. Bergqvist, O. Eriksson, J. Kudrnovsky, V. Drchal, P. Korzhavyi, and I. Turek, *Phys. Rev. Lett.* **93**, 137202 (2004).
- ²⁷H. Raebiger, A. Ayuela, and J. von Boehm, *Phys. Rev. B* **72**, 014465 (2005).
- ²⁸K. Sato, P. H. Dederichs, and H. Katayama-Yoshida, *Europhys. Lett.* **61**, 403 (2003).
- ²⁹J. L. Xu and M. van Schilfhaarde, and G. D. Samolyuk, *Phys. Rev. Lett.* **94**, 097201 (2005).
- ³⁰Yu. Uspenskii, E. Kulatov, H. Mariette, H. Nakayama, and H. Ohta, *J. Magn. Magn. Mater.* **258-259**, 248 (2003).
- ³¹T. Takeuchi, Y. Harada, T. Tokushima, Y. Takata, A. Chainani, J. J. Kim, P. P. Chen, H. Makino, T. Hanada, T. Yao, T. Yamamoto, T. Tsukamoto, K. Kobayashi, and S. Shin, *J. Electron Spectrosc. Relat. Phenom.* **144-147**, 707 (2005).
- ³²L. M. Sandratskii and P. Bruno, *Phys. Rev. B* **67**, 214402 (2003).